Acta Oceanol. Sin., 2023, Vol. 42, No. 10, P. 10–22
https://doi.org/10.1007/s13131-023-2277-4
http://www.aosocean.com
E-mail: ocean2@hyxb.org.cn

Characteristics of extratropical cyclone variability in the Northern Hemisphere and their response to rapid changes in Arctic sea ice

Di Chen[1], Qizhen Sun[2]*

[1] Ocean University of China, Qingdao 266100, China

[2] National Marine Environmental Forecasting Center, Beijing 100081, China

Received 27 October 2022; accepted 1 December 2022

Abstract

Extratropical cyclones are critical weather systems that affect large-scale weather and climate changes at mid-high latitudes. However, prior research shows that there are still great difficulties in predicting extratropical cyclones for occurrence, frequency, and position. In this study, mean sea level pressure (MSLP) data from the European Centre for Medium-Range Weather Forecasts (ECMWF) reanalysis (ERA5) are used to calculate the variance statistics of the MSLP to reveal extratropical cyclone activity (ECA). Based on the analysis of the change characteristics of ECA in the Northern Hemisphere, the intrinsic link between ECA in the Northern Hemisphere and Arctic sea ice is explored. The results show that the maximum ECA mainly occurs in winter over the mid-high latitudes in the Northern Hemisphere. The maximum ECA changes in the North Pacific and the North Atlantic, which are the largest variations in the Northern Hemisphere, are independent of each other, and their mechanisms may be different. Furthermore, MSLP is a significant physical variable that affects ECA. The North Atlantic Oscillation (NAO) and North Pacific Index (NPI) are significant indices that impact ECA in the North Atlantic and North Pacific, respectively. The innovation of this paper is to explore the relationship between the activity of extratropical cyclones in the Northern Hemisphere and the abnormal changes in Arctic sea ice for the first time. The mechanism is that the abnormal changes in summer-autumn and winter Arctic sea ice lead to the phase transition of the NPI and NAO, respectively, and then cause the occurrence of ECA in the North Pacific and North Atlantic, respectively. Arctic sea ice plays a crucial role in the ECA in the Northern Hemisphere by influencing the polar vortex and westerly jets. This is the first exploration of ECAs in the Northern Hemisphere using Arctic sea ice, which can provide some references for the in-depth study and prediction of ECAs in the Northern Hemisphere.

Key words: extratropical cyclones, mean sea level pressure, North Atlantic Oscillation (NAO), North Pacific Index (NPI), Arctic sea ice

Citation: Chen Di, Sun Qizhen. 2023. Characteristics of extratropical cyclone variability in the Northern Hemisphere and their response to rapid changes in Arctic sea ice. Acta Oceanologica Sinica, 42(10): 10–22, doi: 10.1007/s13131-023-2277-4

1 Introduction

An extratropical cyclone is an approximately elliptical baroclinic atmospheric eddy that occurs in mid-high latitudes where the central air pressure is lower than the surroundings and has a cold core that is not the same as that of tropical cyclones. It is an important bridge for the transportation of moisture and momentum to polar regions from low latitudes and plays a critical role in the global climate system. However, extratropical cyclones are usually accompanied by severe weather, such as extreme temperatures, heavy rainfall, severe storms, storm surges, and other meteorological disasters (Averkiev and Klevannyy, 2010; Colle et al., 2015; Feser et al., 2015). It threatens the human living environment, our lives, and property safety. Therefore, it is of great significance to study the temporal and spatial distribution as well as the activity regularity and the variation trend of extratropical cyclones to understand the regional and global climates.

In recent decades, great efforts and progress have been made in the long-term prediction and short-term forecasting of extratropical cyclone activity (ECAs). However, accurately forecasting and predicting ECA is not straightforward, not only because of the variability of extratropical cyclones and the uncertainty in the physical properties of this complex three-dimensional weather system, but also considering that some operational forecasting systems have difficulty providing satisfactory forecasts beyond 7 d due to inherent predictability limitations (Froude, 2011; Marshall et al., 2009; Maycock et al., 2011). Despite the use of weather maps, satellite cloud images and other numerical forecasting products have been extensively analyzed and verified, and the prediction skill still needs to be improved further because of the limitations of data, observations, improper models, and other factors (Bengtsson et al., 2006; Pinto et al., 2006, 2007; Raible, 2007).

Geng and Sugi (2001) used objective methods and reanalyzed data from the European Centre for Medium-Range Weather Forecasts (ECMWF) to study the intensity of the North Atlantic (NA) extratropical cyclone. They realized that there is an increasing trend as a result, which may be related to large-scale baro-

Foundation item: The National Key Research and Development Program of China under contract No. 2022YFF0802002.
*Corresponding author, E-mail: qzsun.tj@foxmail.com

clinic waves in the troposphere and North Atlantic Oscillation (NAO). There is a close relationship between the activity of extratropical cyclones in the Atlantic Ocean in winter and the NAO (Fu et al., 2016). The high-frequency area of extratropical cyclones during the positive phase of a NAO event is moving northward and it is moving southward during the negative phase. The study by Serreze et al. (1997) shows a certain connection between cyclone activity in low-pressure areas of Iceland and NAO. When NAO is significantly negative, the occurrence of cyclones in cold seasons is twice that in normal years, and the intensity decreases, but the location of the cyclone generation and the maximum deepening rate of the cyclone are the same as those in normal years. When the NAO phase is positive, there is no obvious increase in cyclones in Iceland during the cold season, but the cyclone activity in the area north of 60°N increases significantly in both the cold and warm seasons, especially in the Arctic Ocean and the waters near Canada. It is related to the reduced mean sea level pressure (MSLP). Studies have shown that the NAO has interannual and interdecadal variability characteristics (Gong et al., 2002). Its weather-scale variability characteristics are an important factor influencing the interannual variability of extratropical cyclones in the NA (Luo et al., 2012).

In terms of changes in extratropical cyclones in the Northern Hemisphere (NH), an empirical orthogonal function (EOF) analysis of variance statistics of the MSLP of ECA in the North Pacific (NP) and NA was carried out. It was found that the frequency of cyclone activity in North Atlantic/North America had obvious interannual changes, and the overall trend was significant (Zhang et al., 2012). However, the distribution pattern of the EOF at higher latitudes is opposite to that at lower latitudes. The North Atlantic/North American region shows the characteristics of increasing baroclinicity at higher latitudes and weakening baroclinicity at lower latitudes (Hall et al., 2015). This change in baroclinicity of the atmosphere may have caused the shifting characteristics of storm tracks in the North Atlantic/North America to higher latitudes (Knippertz et al., 2000).

Graham and Diaz (2001) used EOF to analyze the climatic characteristics and changes in cyclones in the NP from 1958 to 2011 and found that the frequency and intensity of strong cyclones increased significantly. Favre and Gershunov (2006) used EOF to show that the intensity of extratropical cyclones in the Northeast Pacific region has increased since the 1970s, and the cyclone's path has shifted to the south. The seasonal Aleutian low pressure may cause the positive phase of the interdecadal oscillation in the NP, the positive anomaly of sea surface temperature on the west coast of North America, and the negative anomaly of the central Pacific pressure. In recent decades, scientists have mainly used sea level pressure fields (Lionello et al., 2008; Mendes et al., 2010) or geopotential height fields (Haak and Ulbrich, 1996; Blender et al., 1997) to objectively identify and track extratropical cyclones. These analysis methods have shortcomings, for example, the surface pressure field is often affected by large-scale systems such as the Icelandic low pressure, and fast-moving weak systems are also covered by strong background air currents such as subtropical jets. They cannot be objectively judged and tracked until they develop strongly. Therefore, the index defined by sea level pressure and geopotential height field can be favored for the slow-moving large-scale low-pressure systems (Hoskins and Hodges, 2002). In another way, Wallace et al. (1988) defined ECA by applying a 24-h difference filter using MSLP data called ECApp, shown as follows, where t is any time step of the dataset. Hence ECA is quantified at each grid point by the mean square of the 24-h difference of MSLP. The overbar represents averaging over time, which can be 1 week, 2 weeks, or 1 month.

$$\mathrm{ECA_{pp}} = \overline{\{(\mathrm{MSLP}(t+24\ \mathrm{h}) - \mathrm{MSLP}(t)\}^2}. \tag{1}$$

Its advantage is that the bandpass filter has half power points at periods of 1.2 d and 6 d, which is an extratropical cyclone life cycle, thus highlighting synoptic-scale information variability, and so the 24-h MSLP variation statistics have been widely used to quantify "storminess" (Alexander et al., 2005; Feser et al., 2015). According to previous studies (Wallace et al., 1988), the maxima from this filter usually occur over extratropical cyclone high-frequency regions. Chang and Fu (2002) have shown that this matrix can retain the synoptic time scale well, so variance statistics can be used as an indicator of the ECA.

Based on previous studies, several phenomena can provide sources for ECA predictability, including the El Niño-Southern Oscillation (ENSO), polar vortex, Madden-Julian Oscillation (MJO), and quasi-biennial oscillation (QBO) (Black et al., 2017; DelSole et al., 2017; Garfinkel et al., 2018; Tian et al., 2017; Xiang et al., 2019). ENSO could modulate ECA significantly in NH (Eichler and Higgins, 2006; Zhang and Held, 1999). El Niño events are associated with equatorward and eastward shifts of boreal winter ECA over the Pacific, and ECA over North America weakens, while La Niña events are associated with opposite trends. ECAs over North America can be shifted due to the MJO when tropical diabatic heating is at different locations, but the MJO also has a significant impact on ECAs over the NP, the NA, and North America (Guo et al., 2017; Lee and Lim, 2012) through the MJO-induced Rossby waves that propagate into the mid-latitudes. The QBO generates variability of ECA in the upper troposphere in the NH, and the polar vortex in the NH stratosphere has also been shown to influence ECA (Kidston et al., 2015; Scaife et al., 2012), especially over the NA (Walter and Graf, 2005). Moreover, the midlatitude jet is modulated by stratospheric wind anomalies via the "downward control" mechanism (Haynes et al., 1991), which results in enhanced or suppressed ECA due to stronger or weaker zonal flow.

As we mentioned above, ECA in the NH is influenced by air temperature, air pressure, and atmospheric circulation, especially at high latitudes. On the other hand, the variability of Arctic sea ice has a significant impact on high latitude temperature, pressure field and circulation (Chen and Sun, 2022a; Vihma, 2014). For example, previous studies have shown the role of Arctic sea ice in global atmospheric circulation (Budikova, 2009; Chen and Sun, 2023), the relationship between sea ice and NAO, storms (Bader et al., 2011), and the significant correlation between Greenland sea ice concentration anomalies and the Eurasian mid- and high-latitude atmospheric circulation (Wu et al., 2013). Arctic sea ice variability has a critical impact on mid- and high-latitude climate change, especially on the frequency of winter weather extremes in Eurasia (Chen and Sun, 2022b), but there are few investigations into the analysis of the relationship between ECA and sea ice. The changes in Arctic sea ice could affect the ECA in the NH through some "bridges", but the "bridges" have not received sufficient attention thus far. Meanwhile, the North Pacific Index (NPI) and NAO are indices of the Pacific and Atlantic atmospheric circulation modes, which have significant effects on the climate in the NH at middle and high latitudes, and they will also have some connections to the ECA (Kaplan, 2011). NPI is the average monthly sea level pressure anomaly in the Aleutian low-pressure area near Alaskan Bay (30°–65°N, 160°E–

140°W) (Trenberth and Hurrell, 1994). The main mode of atmospheric circulation in the NP in winter shows the intensity change of the Aleutian Low (AL). NPI is a sensitive index for this mode, which can be used to reveal the variability of the NP sea level pressure in the cold season. Negative (positive) NPI values correspond to stronger (weaker) Aleutian low than average, as well as increased south (north) winds in the eastern Pacific Ocean and warmer (colder) temperatures on the west coast of North America (Allan and Komar, 2006). To date, there has been little research on the relationship between extratropical cyclone activity and the NPI in the NP. Therefore, this paper focuses on the relationship between the NH ECA and Arctic sea ice variability to reveal the potential mechanism between them. Our research intends to provide some references for an in-depth study and prediction of ECA in the NH.

2 Data and methods

2.1 *Data*

The variables adopted include geopotential height, zonal wind (u), meridional wind (v), and vertical wind (w) ranging from 10 hPa to 1 000 hPa, with 17 levels in total as well as MSLP, which come from the ECMWF since it has the highest skill level for nearly all cyclone properties, including cyclone position, intensity, and propagation speed, which is 6 h ERA5 (Hersbach et al., 2020) with a 1°×1° horizontal resolution from 1979 to 2021. Moreover, we also use the monthly NAO index from Climate Prediction Center, NOAA, as well as the monthly NPI from National Center for Atmospheric Research.

According to the relevant description from the data source, the NAO index is based on the surface sea-level pressure difference between the subtropical (Azores region) high and the subpolar low (Iceland), and the NPI is the area-weighted sea level pressure in the region 30°–65°N, 160°E–140°W. Arctic sea ice concentration (ASIC) data were derived from the Hadley Center with a horizontal resolution of 1° × 1° (Rayner et al., 2003) from 1951 to 2021.

2.2 *Methods*

2.2.1 *Calculation of ECApp*

As discussed in the introduction, ECApp is defined by applying a 24-h difference filter on MSLP data (Eq. (1)). The 24-h MSLP change statistics have been widely employed to evaluate "storminess" due to the benefit that the bandpass filter includes half power points at intervals of 1.2 d and 6 d, which is an extratropical cyclone life cycle, highlighting synoptic time scale variability. ECApp could highly correlate with precipitation and extreme wind events in the NH, including parts of North America (Chang et al., 2015; Ma and Chang, 2017) and much of Europe (Yau and Chang, 2020). Thus, the variance statistics of MSLP (ECApp) can be a good measure of ECA.

2.2.2 *EOF analysis*

EOF analyses are often used to study possible spatial patterns of climate variability and how they change with time (Hannachi et al., 2007). In statistics, one can project the original climate data on an orthogonal basis, which is derived by computing the eigenvectors of a spatially weighted anomaly covariance matrix, and the corresponding eigenvalues provide a measure of the percent variance explained by each pattern. Therefore, we use EOF analysis to represent the spatial distribution and temporal changes in ECA in our research.

2.2.3 *Pearson correlation analysis*

The proportion of the total variance in the observed data that can be described by a linear model of the research variables is expressed by Pearson's product-moment correlation coefficient, also known as the Pearson coefficient. The value can be anywhere between –1 and 1, with greater absolute values suggesting stronger interdependence between the variables (Benesty et al., 2009). Here, we adopt this method to demonstrate the relationship between ECA and NAO in the Atlantic sector and the linkage between ECA and NPI in the Pacific sector, as well as the potential links between ECA and Arctic sea ice.

2.2.4 *Composite analysis*

Composite analysis, also referred to as superposed epoch analysis and conditional sampling, is a useful tool to help understand the relationships among different phenomena and determine some of the basic structural characteristics of a meteorological or climatological phenomenon that are difficult to observe in totality (Haurwitz and Brier, 1981; Laken and Čalogović, 2013). We use the method to explain the internal connection between the NPI and the NP ECA.

2.2.5 *Singular value decomposition (SVD) analysis*

SVD is a factorization of a real or complex matrix in linear algebra. It applies the orthonormal eigenbasis square normal matrix's eigendecomposition to any $m \times n$ matrix (Kalman, 1996). It is connected to polar decomposition and used in meteorology to examine the interactions between two fields.

2.2.6 *Calculation of the polar vortex index*

The 550-dam contour of 500 hPa geopotential height is used to define the southern boundary of the polar vortex in the Pacific sector using the definition of the polar vortex by the National Climate Center of China Meteorological Administration (http://cmdp.ncc-cma.net/).

3 Results and discussion

3.1 *The climatology and monthly standard deviation of the extratropical cyclones in the NH*

Figure 1 shows the variation of the ECA climatology (Fig. 1a) and standard deviation (Fig. 1b) in the NH, from which it can be seen that the maximum value of the annual variation of climatology occurs in winter (from December to February) (49.6 hPa^2, 48.2 hPa^2, 46.8 hPa^2), while the minimum value occurs in summer (from June to August) (17.6 hPa^2, 14.6 hPa^2, 17.1 hPa^2). The maximum value of the standard deviation also occurs in winter (66.4 hPa^2, 64.8 hPa^2, 63.3 hPa^2), while the minimum occurs in summer (23.9 hPa^2, 19.3 hPa^2, 23.2 hPa^2)

3.2 *Multiyear mean variability of extratropical cyclones in the NH*

Figure 2 shows the spatial climatology and standard deviation distribution of ECA in NH from 1979 to 2021.

The multiyear mean and winter ECAs mainly occur in the middle and high latitudes in the NH (Figs 2a and b). The maximum in the NH primarily appears in the NP and the NA, both in the multiyear mean and winter, which are 85 hPa^2 and 140 hPa^2, respectively.

Figures 2c and d show the standard deviation distribution characteristics of ECA in the multiyear mean and winter. Through comparative analysis, the pattern is similar to the multiyear mean (Fig. 1). The multiyear and winter maximum standard deviations in the NH both appear in the NP and NA, which are

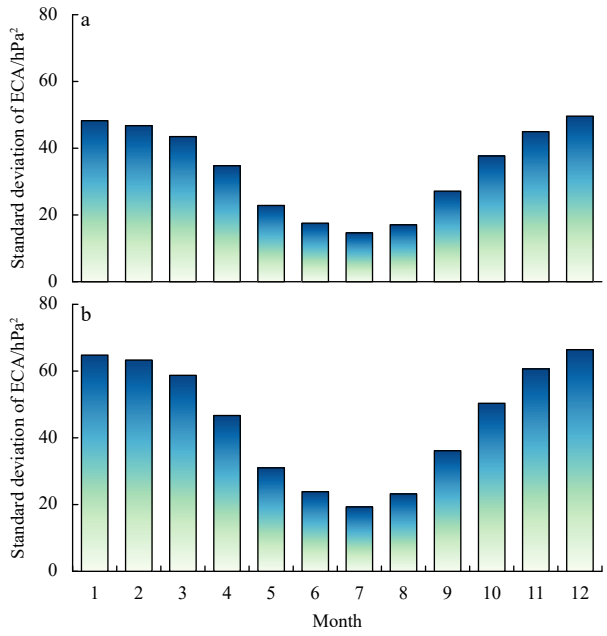

Fig. 1. The monthly climatology (a) and standard deviation (b) of the ECA in the NH for 1979–2021.

140 hPa^2 and 170 hPa^2, respectively. The value in winter is higher than that in multiple years.

The above analysis shows that ECA mainly occurs in winter. Therefore, we will next focus on the characteristics of ECA changes in winter.

To further determine the temporal and spatial variation characteristics of extratropical cyclones in the NH, EOF analysis is applied to investigate the ECA of winter in the NH from 1979 to 2021. The results show that the contribution of the first mode of ECA in the NH is 19.5%, and the contribution of the second mode is 14.5% (Fig. 3).

It is shown that the spatial distribution of the first mode of ECA in the NH is mainly a quasi-Arctic Oscillation (AO) pattern. The second mode is centered on the North Pole, forming a dipole with the NA and NP. Meanwhile, Fig. 3c shows that the ECA temporal distribution of the first mode slightly increases from 1979 to 2021, whereas the ECA spatial pattern of the second mode demonstrates a weak decreasing trend during the period in Fig. 3d. Moreover, according to the correlation analysis of ECA and MSLP (Fig. 4), the changes of ECA are closely related to the changes of MSLP in the NH, and the high correlation can be seen in the high-frequency region of ECA in NP and NA. This shows that MSLP variations make a vital contribution to ECA, which is consistent with the prior result (Hannachi et al., 2007).

3.3 *The relationship between NAO and ECA in the NH*

The analysis of monthly ECA and NAO in the winter from 1979 to 2021 in the NH using the above calculation methods (Fig. 5a) shows that the high correlation between NAO and ECA changes occurs in the NA, North America to Greenland, and the Eurasian continent, while there is a negative correlation between these two in the Asia-Europe region and the southeastern United States. There is also a positive correlation between them in the Arctic region. Figure 5a depicts the dipole mode for the ECA in the NA as well, and Fig. 3b's dipole mode between the NP and the Arctic-Pacific sector can be explained by the location of the strong baroclinicity region and the westerly belt position, as Fu et al. (2016) discovered for the dipole mode between the NA and the Arctic-Atlantic sector.

It can be explained that the NAO has an important effect on the change of the ECA in the North Atlantic, but the opposite process is observed in the Arctic. That is, ECA appears to be less in the North Atlantic when the NAO has a positive anomaly, while ECA tends to increase in the Arctic. The mechanism is that when the NAO is a positive anomaly, ECA will increase due to low pressure in high latitudes and decrease due to high pressure in mid-latitudes. In addition, due to an increase in the north-south pressure difference, the meridional circulation is strengthened and the westerly flow is strengthened and moved northward, which in turn leads to more high-latitude ECAs and vice versa (Chiang et al., 2014; Fu et al., 2016; Yang et al., 2022).

3.4 *The relationship between NPI and ECA in the NH*

As far as current research is concerned, the use of NPI to study ECA is limited. As mentioned earlier, the maxima of ECA occur mainly in the NP and NA, and the changes between them are independent. Thus, we speculate that the changes in the NP ECA may be related to the NP MSLP since the results of the analysis in Fig. 4 indicate that ECA is closely related to MSLP. For this reason, we use the NPI that reflects the changes in the MSLP pressure field in the NP to analyze and explore its relationship with the NP ECA.

Figure 5b shows the correlation field between ECA in NH and NPI in winter. The high correlation between ECA and NPI is located in the NP and Arctic-Pacific sectors and central North America, and it shows an obvious dipole pattern. When the NPI has a positive (negative) anomaly, the NP ECA will have a negative (positive) anomaly, and the Arctic-Pacific sector and the ECA in central North America will have a positive (negative) anomaly. The results of this analysis show that the variations of ECA in the NP and Arctic-Pacific sectors, as well as the central United States, are strongly affected by the NPI.

To explain the internal relationship between the NPI and ECA in the NP, we selected the 850-hPa geopotential height and u and v wind components corresponding to the positive and negative NPI maximum anomaly years from 1979 to 2019, respectively, for composite analysis.

Figure 6 shows the composite analysis of the 850-hPa geopotential height as well as the wind vector field corresponding to NPI positive anomaly and negative anomaly. Figure 6a shows the geopotential height and wind vector field corresponding to the NPI positive anomaly years. When the NPI is in positive anomaly years, the geopotential height of the NP Ocean is obviously high, and a strong anticyclonic circulation appears. On the east side of the anticyclonic circulation, there is a southward airflow, and the southward dry and cold airflow has been driven from high latitudes to mid-latitudes. Figure 6b shows the geopotential height and wind vector field corresponding to the NPI negative anomaly years. When the NPI is in negative anomaly years, the geopotential height of the NP Ocean is obviously low, and strong cyclonic circulation appears. On the east side of the cyclone circulation, there is a southerly airflow, and the northward warm and humid airflow is affected by the mid-latitude of the Pacific Ocean to the high latitudes.

With the geopotential height and anticyclone (cyclone) circulation field corresponding to the NPI positive and negative anomalies reflected in Figs 6a and b, this circulation will affect the occurrence of ECA in the NP through the meridional dry and cold (warm and wet) air currents, respectively. When the NPI is a positive (negative) anomaly, the geopotential height of the NP is

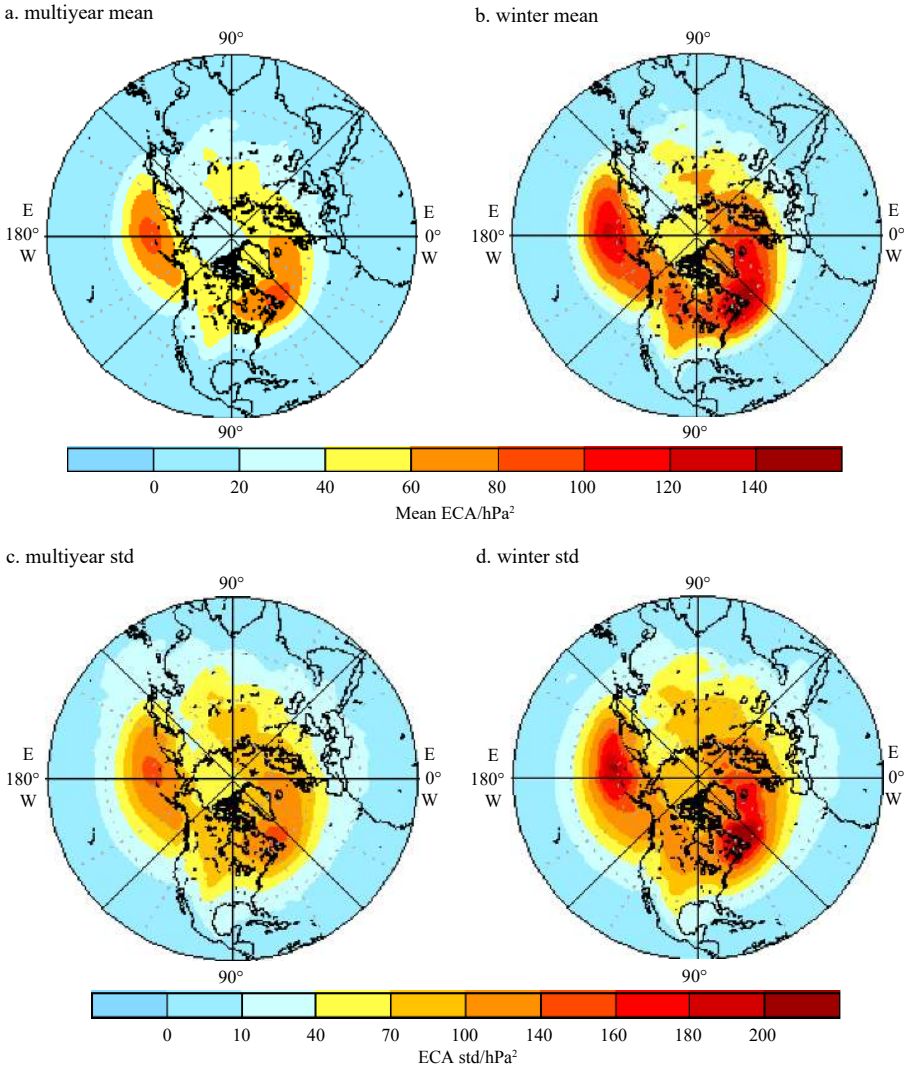

Fig. 2. The multiyear mean (a) and winter mean (b) distribution of ECA and multiyear (c) and winter (d) standard deviation (std) of ECA over the NH for 1979–2021 based on ERA5 reanalysis daily MSLP data.

higher (lower), and the anticyclone (cyclone) circulation guides the high (middle) latitude dry and cold (warm and wet) airflow to the south (north), leading to a decrease (increase) of frontal activity in the mid-high latitudes of the NP, which eventually results in less (more) ECA in the NP.

3.5 *Linkage between extratropical cyclones and Arctic sea ice*

To understand the connection between the Pacific ECA and Arctic sea ice, we conducted an SVD analysis of the Pacific ECA in winter and Arctic sea ice in summer and autumn from 1979 to 2021, and the coupling results between them are shown in Fig. 7. There is a close relationship between the Pacific ECA in winter and the Arctic sea ice changes in summer and autumn. From the spatial distribution of SVD, the Pacific ECA shows the inverse phase variation in middle and high latitudes corresponding to the inverse phase variation in the Pacific sector and the Atlantic sector of the Arctic sea ice. The results of this Pacific ECA spatial distribution are consistent with Zhang et al. (2012), while the dipole distribution of the Arctic sea ice spatial distribution is similar to the Arctic dipole (Overland and Wang, 2010; Chen et al., 2016). The most significant regions for the coupling of the two variables are mainly the Beaufort Sea, Chukchi Sea, East Siberian Sea and the Laptev Sea in the Pacific sector, as well as around Greenland and north of the NP and the Aleutian Islands. In addition, the spatial distribution of the coupling of the two variables shows that when there is a positive (negative) anomaly in Arctic sea ice in summer and autumn, there is more (less) ECA in the Pacific Ocean at mid-latitudes and less (more) ECA at high latitudes. The coupling time series of the two variables show that they both have the same phase change relationship, and the correlation is significant (r = 0.72). That is, when there is anomalously more (less) sea ice in summer and autumn, the Pacific ECA will be anomalously more (less). From 1979–2021, both summer-autumn Arctic sea ice and ECA show a decreasing trend, while the decreasing rate of summer-autumn sea ice is slightly larger than that of Pacific winter ECA.

The seasonal and annual characteristics of extratropical cyclones in the NH have been analyzed and explored in the previous section, revealing that extratropical cyclones in the NH mainly occur in winter, and their maximum frequency occurs in the NP and NA. The NPI and NAO are the critical factors affecting the occurrence of extratropical cyclones in the NP and NA, respectively. Therefore, this section will focus on analyzing and exploring the link between the abnormal changes of NPI and NAO and Arctic

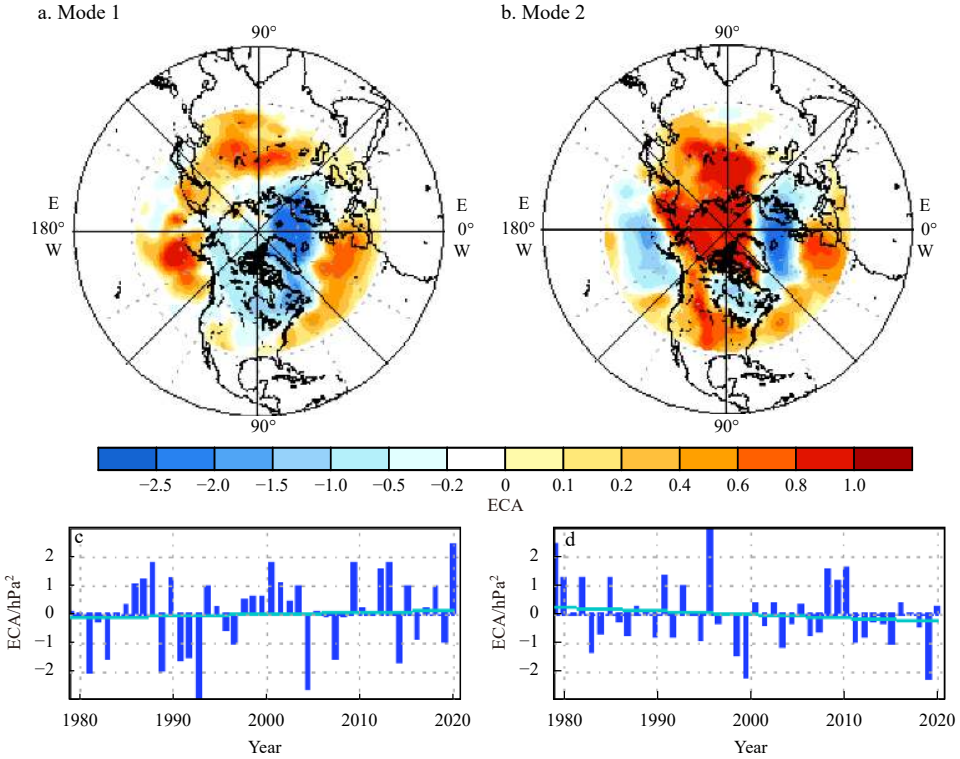

Fig. 3. The EOF spatial patterns and the time series of ECA in the NH in winter (from December to February). a and b are spatial patterns of the Mode 1 (19.5% of the total variance) and the Mode 2 (14.5% of the total variance); c and d are the time series of the Mode 1 and Mode 2.

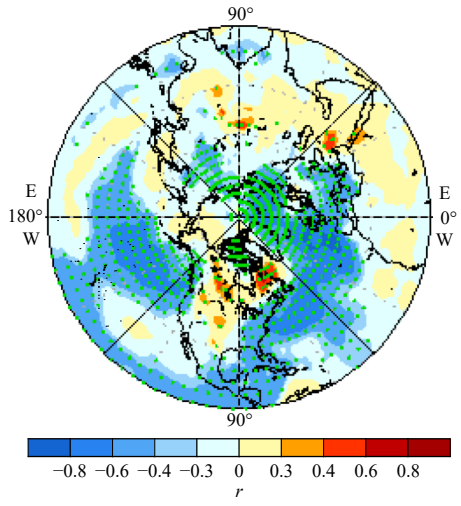

Fig. 4. The spatial distribution of correlation coefficient (r) between ECA and MSLP in the NH in winter. The green dots are significant at the 95% confidence level (t-test).

sea ice, expecting to reveal the mechanism of extratropical cyclone generation in the NH.

To reveal whether there is a link between Arctic sea ice and the NPI and NAO, the monthly Arctic sea ice concentration (ASIC) data from 1951–2021 are used for analysis with the NPI and NAO. Considering that Arctic sea ice has a melt season in summer-autumn and a freezing season in winter each year, there is a close relationship between sea ice changes in these two different seasons and climate (Francis et al., 2009; Ghatak et al., 2010). Therefore, summer-autumn and winter sea ice anomaly changes are selected as the key seasons for analysis to explore the linkage with the NPI and NAO. Figure 8 shows the correlation fields between summer-autumn Arctic sea ice and NPI and winter Arctic sea ice and NAO, and it can be seen that the sea ice changes that are strongly correlated with NPI and NAO are both in the Pacific sector (reaching the 95% confidence level), the Chukchi Sea and the Beaufort Sea. Figure 8a shows the correlation field between Arctic summer and autumn sea ice and winter NPI, which have an inverse phase correlation. Figure 9b shows the correlation field between winter sea ice and winter NAO, and there is the same phase correlation between them. This relationship indicates that when there is an abnormally high (low) amount of sea ice in summer and autumn, there will be an abnormally low (high) change in the NPI in the winter of that year. In contrast, when there is an abnormally high (low) amount of sea ice in winter, there is a positive (negative) change in the NAO phase in winter of that year.

Further studies have revealed that in different seasons, the abnormal sea ice in the key Arctic region influences ECA over the different regions. The key area in Fig. 8a (green area) is the high correlation field for winter NPI and summer/fall ASIC; the key area in Fig. 8b (green area) is the high correlation field for winter NAO and winter ASIC. Figures 9a and b show the composite 500-hPa geopotential height field reflecting the spatial distribution of geopotential height anomalies as well as polar vortex and jet stream intensity changes for anomalously more (less) sea ice in the Arctic key region in summer and autumn. That is, when the Arctic key area sea ice has positive anomalies in summer and autumn, there are significant negative anomalies in geopotential height in the NP region, and positive anomalies in Eurasia, North America and the Nordic continent. Anomalous low pressure will occur at sea surface level in the NP, and ECA will increase. When the Arctic key area sea ice is a negative anomaly in summer and

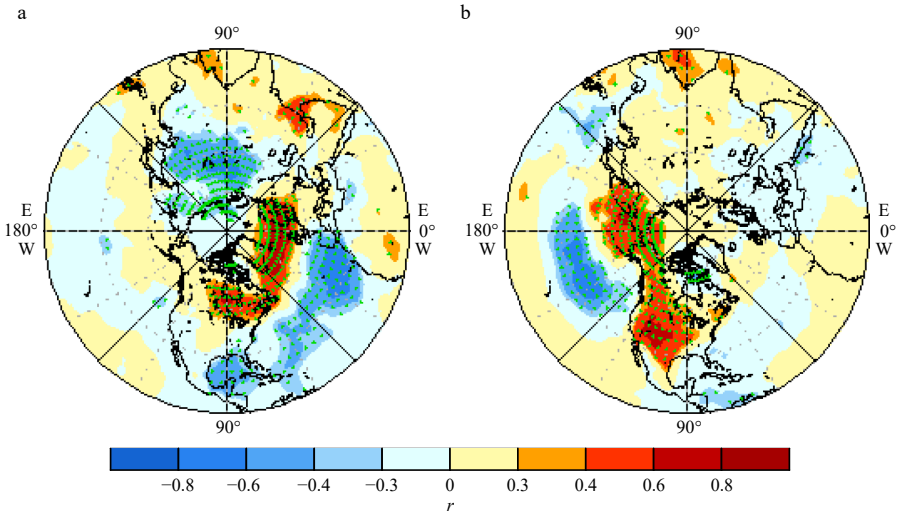

Fig. 5. The spatial patterns of the correlation coefficient (r) between ECA and NAO (a) and the correlation coefficient between ECA and NPI (b) in winter (from December to February). The green dots are significant at the 95% confidence level (t-test).

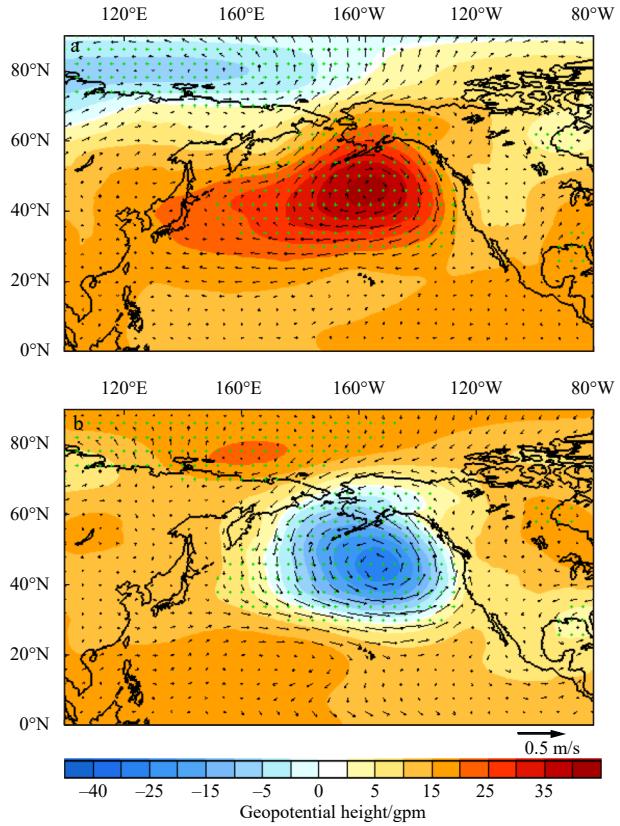

Fig. 6. Composite analysis of 850-hPa geopotential height (shaded, unit in gpm) and circulation (vector), in which NPI is an anomaly in winter (from December to February). a. The geopotential height when NPI is a positive phase; b. the geopotential height when NPI is a negative phase. The green dots denote the regions above the 95% confidence level .

autumn, the NP region shows a significant positive anomaly in geopotential height, and the Eurasian, North American and Nordic continents show a negative anomaly. Anomalous high pressure will occur on the NP sea surface, and ECA will decrease.

In addition, when there is a positive anomaly of sea ice in the key area in summer and autumn, the position of the southern boundary of the polar vortex in the Pacific sector is southward, and the westerly jet stream in the Pacific Ocean is strengthened and expands southward and eastward. When negative anomalies occur in the key area in summer and autumn, the position of the southern boundary of the Pacific sector polar vortex is northward, and the Pacific westerly jet stream is weakened and moves northward and westward.

The strengthening and weakening of the Pacific westerly jet stream play an important role in the Pacific ECA (Luo et al., 2007; Sanders and Gyakum, 1980; Yoshida and Asuma, 2004), and when the jet stream strengthens and moves southward, the NP ECA becomes more frequent (Kobashi et al., 2019). When the Pacific jet stream weakens and withdraws northward, the NP ECA decreases. This result suggests that there is an important influence of Arctic sea ice change in the key areas in summer and autumn on the Pacific ECA and that the polar vortex and westerly jets are important mechanisms leading to ECA in the Pacific region during winter.

However, as mentioned previously, in different seasons, the abnormal sea ice in the key Arctic region influences ECA over the different regions. Figures 9c and d show the spatial distribution of the composite 500-hPa potential height field reflecting the potential height anomalies as well as the changes in the intensity of the polar vortex and jet streams for the anomalously more (less) sea ice in the Arctic key region in winter. When anomalously more or less sea ice occurs in the key Arctic region in winter, the 500-hPa geopotential height field appears to have a completely opposite spatial distribution, similar to the positive and negative NAO phases (Donat et al., 2010). When there is a positive anomaly of sea ice in the key area during wintertime, the southern boundary of the polar vortex in the Atlantic sector northward and the North American jet streams are weakened and shift northward. When there is a negative sea ice anomaly in the key area in winter, the southern boundary of the Atlantic sector polar vortex is southward, and the North American jet stream strengthens and moves southward.

The mechanism of the influence of the North American westerly jet on the Atlantic ECA is the same as that of the Pacific westerly jet on the Pacific ECA. In other words, when the jet strengthens and moves south, the mid-latitude ECA will become more frequent, while the high latitude ECA will decrease. When the jet

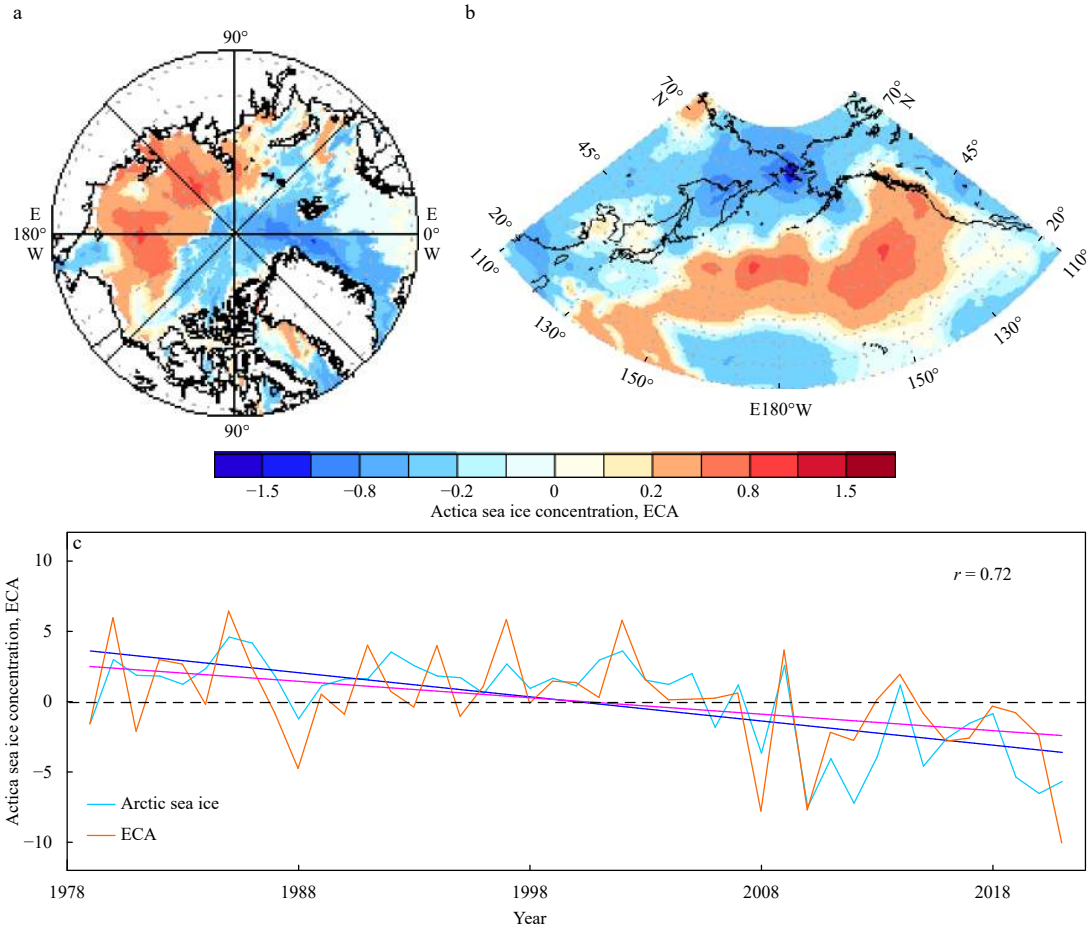

Fig. 7. SVD analysis of the Arctic sea ice in the summer-autumn and Pacific ECA in winter. a. Arctic sea ice; b. ECA; c. time series of the Arctic sea ice and Pacific ECA. The blue and red lines are the linear trends of the Arctic sea ice and ECA, respectively.

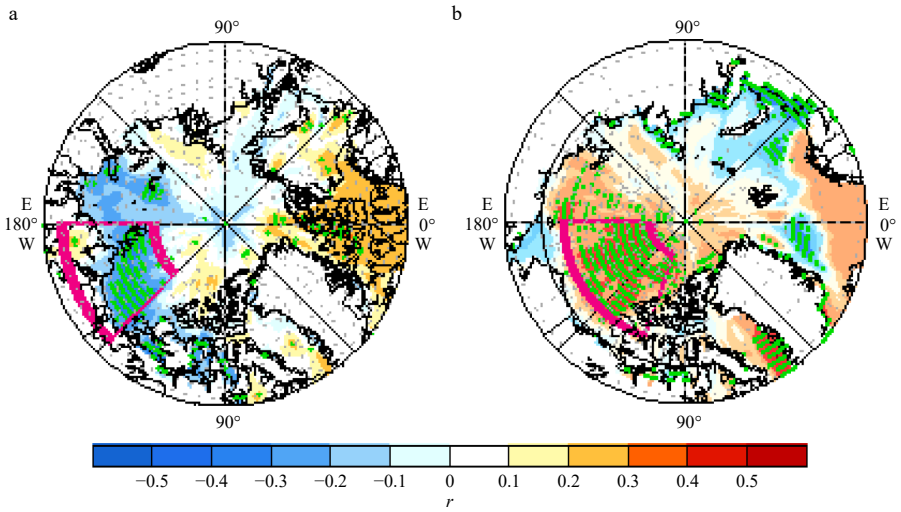

Fig. 8. The spatial distribution of correlation coefficient (r) between ASIC and NPI and the correlation coefficient between ASIC and NAO. a. The correlation between the NPI in ASIC in summer-autumn; b. the correlation between the NAO in winter and the ASIC in winter. The magenta fan frame denotes the key area. The green dots denote the regions above the 95% confidence level.

stream weakens and withdraws northward, the mid-latitude ECA will decrease, while the high-latitude ECA will increase. From this, it can be concluded that Arctic sea ice changes in the key region during winter have an important influence on the Atlantic ECA.

To further analyze the process of sea ice changes in the Arctic key region on NPI and NAO, a total of 43 years of Arctic sea ice and MSLP data from 1979–2021 were selected based on the criterion of anomalous changes in Arctic sea ice up to one standard deviation, and years of positive and negative anomalies in the key

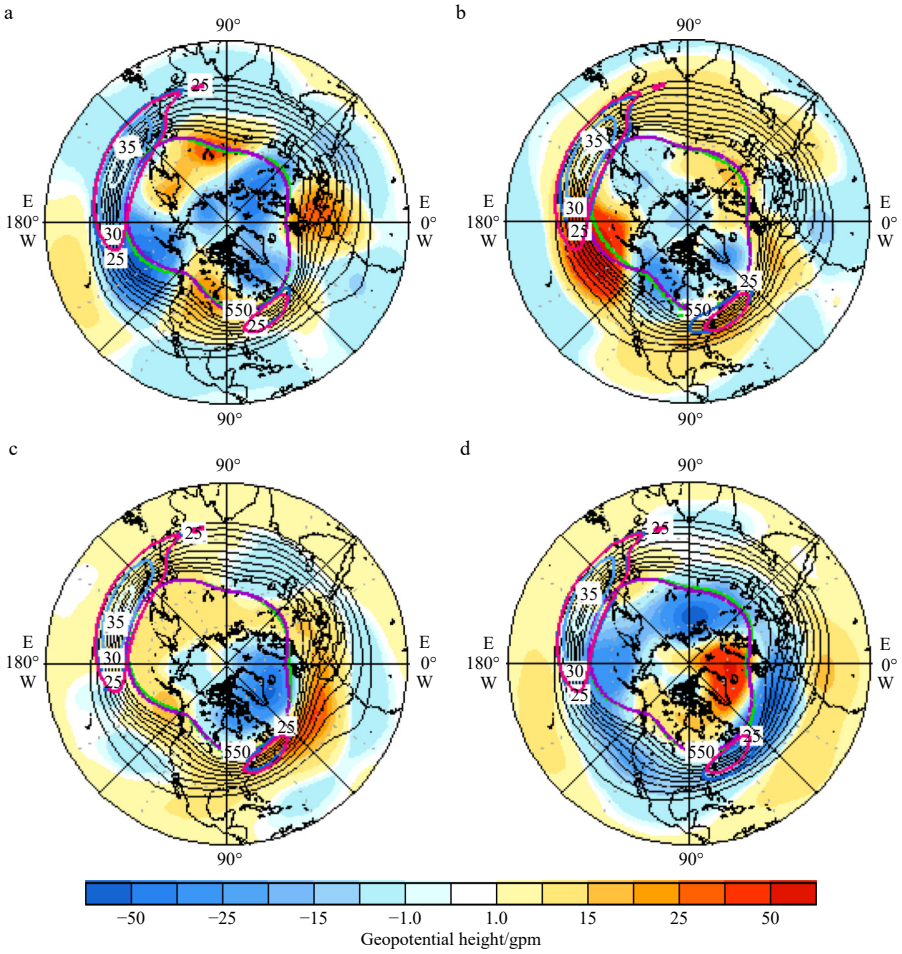

Fig. 9. Spatial distribution of the geopotential height anomaly, polar vortex intensity, and westerly jet intensity at 500-hPa corresponding to the key area ice variation anomaly in summer and autumn (a, b) and winter (c, d). The distribution corresponding to the positive sea ice anomaly (a, c); the distribution corresponding to the negative sea ice anomaly (b, d). The purple closed curve is the climatology of the polar vortex range in winter (550 gpm), and the green closed curve is the polar vortex variation corresponding to the more (less) sea ice in the key area (550 gpm) . The contour lines demonstrate the geopotential height field of the jet stream (560 gpm, 564 gpm, 568 gpm, 572 gpm, 576 gpm, 580 gpm, 584 gpm, 588 gpm and 592 gpm). The blue closed curves reflect the maximum wind speed of the jet (m/s).

region sea ice and the corresponding winter MSLP in NH were selected for composite analysis. Figure 10 shows the spatial distribution characteristics of the NH MSLP, the meridional circulation, and the time-series variation curves of the Arctic sea ice and NPI in the key region corresponding to the positive (negative) anomalies of the Arctic sea ice. When the sea ice in the key region of the Arctic is a positive anomaly, the negative anomaly MSLP in the NP region is obvious, while the sea ice in the key region is a negative anomaly, the positive anomaly sea level pressure field in the NP region is obvious. The regions with positive and negative anomalies of MSLP extremes in the NP region happen to be the regions where ECA occurs most frequently. Figures 10c and d show the altitude-longitude profiles after latitudinal averaging (170°–135°W). In the altitude-longitude profile, when the Arctic sea ice is a positive anomaly, a positive anomaly appears in the high latitude pressure, while a negative anomaly appears in the middle and low latitudes, with a sinking flow at high latitudes, an updraft at middle latitudes, and a strong cyclonic circulation at middle and low latitudes. In the altitude-longitude profile, when Arctic sea ice is a negative anomaly, negative anomalies appear in the high latitude pressure, while positive anomalies appear in the middle latitudes, with updrafts at high latitudes, downdrafts at middle latitudes, and a strong anticyclonic circulation at middle and low latitudes.

Figure 11a shows the long-term variation of sea ice anomalies in the Arctic key region and the NPI variation. It can be found that there is an obvious inverse phase relationship between them, and when there is abnormally high (low) sea ice in the Arctic key region, there will be a negative (positive) anomaly in the NPI, which will lead to a high (low) frequency of the NP extratropical cyclone.

Similarly, the analysis of sea ice changes in the Arctic winter key region and winter NAO shows that there is a positive correlation between them, i.e., when there is more (less) sea ice in the key region in winter, there will be positive (negative) changes in the NAO phase in winter, and the positive (negative) NAO phase has an important role in stimulating extratropical cyclone outbreaks in the NA, resulting in the less (more) frequent occurrence of extratropical cyclones in the NA (Fig. 11b).

4 Conclusions

In summary, the maximum value of the multiyear mean and

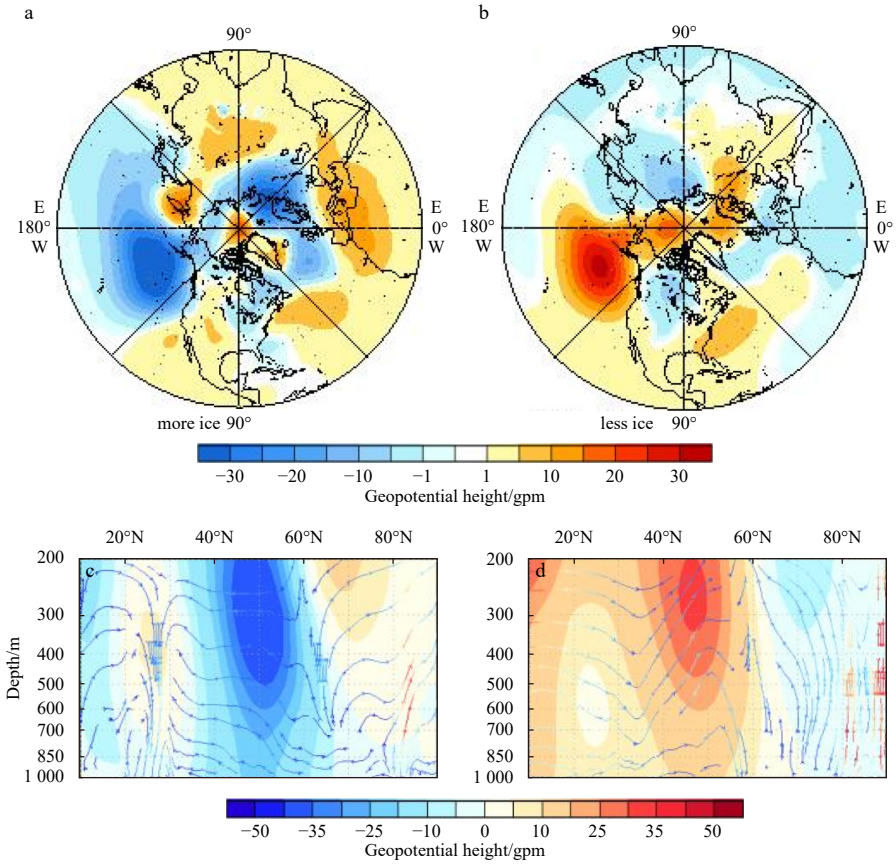

Fig. 10. The results of a composite analysis of more ice years and less ice years. a and b are the NH MSLP corresponding to more and less sea ice in the key area, respectively. c and d are the average profiles in the latitudes 170°–135°W corresponding to more and less sea ice in the key area, respectively. The streamlines mean a two-dimensional wind field at the high-latidude section, where the arrow indicates the rise or fall of the airflow.

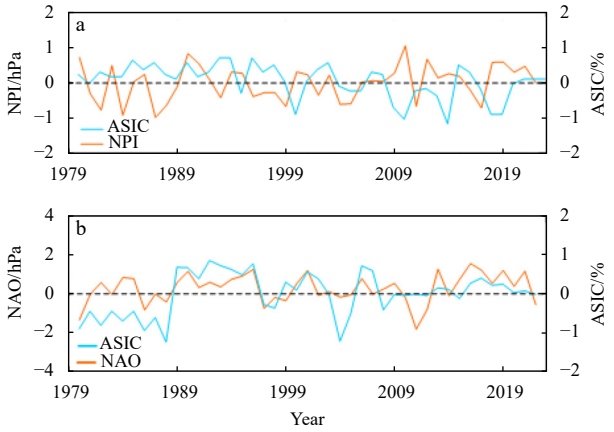

Fig. 11. The variation curves of summer-autumn ASIC in the key area and NPI in winter (a). The variation curves of winter ASIC in the key area and NAO in winter (b).

standard deviation of ECA occurs in the winter in the middle and high latitudes of the NH. The ECA changes in the NH mainly occur in the NP and NA regions, with the highest frequency occurring in winter. The MSLP anomaly is an important factor that affects the frequency and region of ECA. The spatial distribution characteristic of the first mode of ECA in the NH is mainly a quasi-AO pattern. The spatial distribution characteristic of the second mode of ECA is centered on the North Pole and forms a dipole with the NA and NP, respectively. The time series trends of the first and second modes for ECA in NH are both not obvious from 1979 to 2021.

The ECA maximal variations in the NP and the NA are independent of each other. The trend of the largest variance area of ECA in the NP is small, while the trend of the largest variance area of ECA in the NA shows a slight decrease. The ECA in the Atlantic sector (middle latitude and high latitude) and Eurasia are mainly affected by the same period of NAO, and the ECA in the NP and the Arctic in Pacific sectors, as well as the central United States, are mainly affected by NPI.

The process of NAO influence on the NA ECA is mainly through the changes in the pressure field affecting the ECA variations in the middle and high latitudes. In addition, the NAO change anomaly can affect the meridional circulation variation, which will lead to the strengthening (weakening) of the westerly jet and the southern (northern) movement, which ultimately affects the spatial distribution of ECA.

The influence of the NPI on ECA in the NP mainly affects the higher (lower) geopotential height field in the NP, which tends to form anticyclonic (cyclonic) circulation and then influences the frontal activity at mid-high latitudes through the meridional dry and cold (warm and wet) air currents. This process eventually leads to a decrease (increase) of ECA in the NP.

The maximum ECA in the NH is located in the NP Ocean and the NA Ocean, and there are different mechanisms of ECA in these two regions. The ECA in the NP region is mainly influenced

by the NPI, while the ECA in the NA region is mainly influenced by the NAO. In turn, the ECAs in the NP and NA are closely related to the sea ice in the key Arctic regions during different seasons. The ECA in the NP is mainly related to Arctic sector sea ice changes in early summer and autumn, while the ECA in the NA is mainly related to sea ice in the key Arctic regions in winter.

The physical mechanism by which abnormal changes in Arctic sea ice affect NP and NA extratropical cyclones can be explained as follows respectively. When there are positive anomalies (negative anomalies) in summer and autumn sea ice, there are negative anomalies (positive anomalies) in the pressure gradient of mid-high latitudes, and the NPI shows a negative phase (positive phase) and the AO shows a negative phase (positive phase), resulting in the increase (decrease) of ECA in the NP. When the winter sea ice has a positive anomaly (negative anomaly), the Polar vortex has a positive anomaly (negative anomaly), the NAO shows a positive phase (negative phase), and the strength of the Polar Front Jet stream shows a positive anomaly (negative anomaly), resulting in an increase (decrease) of NA ECA (Fig. 12).

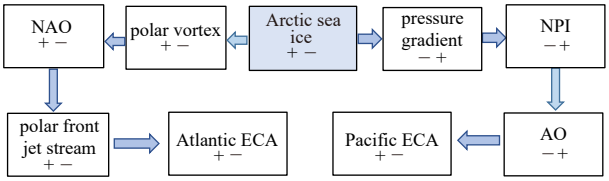

Fig. 12. The linkage between Arctic sea ice variability and the NH ECA. "+" and "–" indicate positive and negative anomalies.

The innovation of this paper is reflected in the first exploration of the relationship between the occurrence of tropical cyclones in the Northern Hemisphere and the abnormal changes of Arctic sea ice, and it is proposed that the abnormal changes of Arctic sea ice are an important mechanism causing ECA in the NP and NA. This will provide a theoretical basis for the further study and prediction of extratropical cyclones. However, there are still some unresolved issues in this paper. Although statistical analysis is used to propose the potential mechanism, such as the influence of the NPI on the ECA in the NP, it is still necessary to use numerical models for investigation in the next step.

Acknowledgements

We thank the data mentioned above and computing resource providers.

References

Alexander L v, Tett S F B, Jonsson T. 2005. Recent observed changes in severe storms over the United Kingdom and Iceland. Geophysical Research Letters, 32. https://doi.org/10.1029/2005GL022371

Allan J C, Komar P D. 2006. Climate controls on US West Coast erosion processes. Journal of Coastal Research, 22(3): 511–529

Averkiev A S, Klevannyy K A. 2010. A case study of the impact of cyclonic trajectories on sea-level extremes in the Gulf of Finland. Continental Shelf Research, 30(6): 707–714, doi: 10.1016/j.csr.2009.10.010

Bader J, Mesquita M D S, Hodges K I, et al. 2011. A review on Northern Hemisphere sea-ice, storminess and the North Atlantic Oscillation: Observations and projected changes. Atmospheric Research, 101(4): 809–834, doi: 10.1016/j.atmosres.2011.04.007

Benesty J, Chen Jingdong, Huang Yiteng, et al. 2009. Pearson correlation coefficient. In: Cohen I, Huang Yiteng, Chen Jingdong, et al, eds. Noise Reduction in Speech Processing. Berlin: Springer, doi: 10.1007/978-3-642-00296-0_5

Bengtsson L, Hodges K I, Roeckner E. 2006. Storm tracks and climate change. Journal of Climate, 19(15): 3518–3543, doi: 10.1175/JCLI3815.1

Black J, Johnson N C, Baxter S, et al. 2017. The predictors and forecast skill of Northern Hemisphere teleconnection patterns for lead times of 3–4 weeks. Monthly Weather Review, 145(7): 2855–2877, doi: 10.1175/MWR-D-16-0394.1

Blender R, Fraedrich K, Lunkeit F. 1997. Identification of cyclone-track regimes in the North Atlantic. Quarterly Journal of the Royal Meteorological Society, 123, 727–741. https://doi.org/10.1002/qj.49712353910

Budikova D. 2009. Role of Arctic sea ice in global atmospheric circulation: a review. Global and Planetary Change, 68(3): 149–163, doi: 10.1016/j.gloplacha.2009.04.001

Chang E K, Fu Y. 2002. Interdecadal variations in Northern Hemisphere winter storm track intensity. Journal of Climate, 15(6): 642–658,

Chang E K M, Zheng Cheng, Lanigan P, et al. 2015. Significant modulation of variability and projected change in California winter precipitation by extratropical cyclone activity. Geophysical Research Letters, 42(14): 5983–5991, doi: 10.1002/2015GL064424

Chen Di, Gao Shanhong, Chen Jinnian. 2016. Impact of the Indo-Pacific warm pool SST anomaly on Arctic sea ice variation. Chinese Journal of Polar Research (in Chinese), 28(1): 49–57

Chen Di, Sun Qizhen. 2022a. Impact of global tropical sea surface temperature anomalies on the Arctic sea ice variation. Haiyang Xuebao (in Chinese), 44(12): 42–54

Chen Di, Sun Qizhen. 2022b. Impact of rapid Arctic sea ice decline on China's crop yield under global warming. Environment, Development and Sustainability, 1–18, https://doi.org/10.1007/s10668-022-02757-x[2022-11-24]

Chen Di, Sun Qizhen. 2023. Northern Pacific extratropical cyclone variability and its linkage with Arctic sea ice changes. Climate Dynamics, 61(11): 5875–5885

Chiang J C H, Lee S Y, Putnam A E, et al. 2014. South Pacific Split Jet, ITCZ shifts, and atmospheric north–south linkages during abrupt climate changes of the last glacial period. Earth and Planetary Science Letters, 406: 233–246, doi: 10.1016/j.epsl.2014.09.012

Colle B A, Booth J F, Chang E K M. 2015. A review of historical and future changes of extratropical cyclones and associated impacts along the US east coast. Current Climate Change Reports, 1: 125–143, doi: 10.1007/s40641-015-0013-7

DelSole T, Trenary L, Tippett M K, et al. 2017. Predictability of week-3–4 average temperature and precipitation over the contiguous United States. Journal of Climate, 30(10): 3499–3512, doi: 10.1175/JCLI-D-16-0567.1

Donat M G, Leckebusch G C, Pinto J G, et al. 2010. Examination of wind storms over Central Europe with respect to circulation weather types and NAO phases. International Journal of Climatology, 30(9): 1289–1300, doi: 10.1002/joc.1982

Eichler T, Higgins W. 2006. Climatology and ENSO-related variability of North American extratropical cyclone activity. Journal of Climate, 19(10): 2076–2093, doi: 10.1175/JCLI3725.1

Favre A, Gershunov A. 2006. Extratropical cyclonic/anticyclonic activity in North-Eastern Pacific and air temperature extremes in western North America. Climate Dynamics, 26, 617–629. https://doi.org/10.1007/s00382-005-0101-9

Feser F, Barcikowska M, Krueger O, et al. 2015. Storminess over the North Atlantic and northwestern Europe—a review. Quarterly Journal of the Royal Meteorological Society, 141(687): 350–382, doi: 10.1002/qj.2364

Francis J A, Chan Weihan, Leathers D J, et al. 2009. Winter Northern Hemisphere weather patterns remember summer Arctic sea-ice extent. Geophysical Research Letters, 36(7): L07503, doi: 10.1029/2009GL037274

Froude L S R. 2011. TIGGE: comparison of the prediction of southern hemisphere extratropical cyclones by different ensemble prediction systems. Weather and Forecasting, 26(3): 388–398, doi: 10.1175/2010WAF2222457.1

Fu Qiang, Zhong Linhao, Luo Dehai. 2016. Characteristics of extratropical cyclone activity at North America-Atlantic area in winter and its relationship with NAO. Marine Science Bulletin (in Chinese), 35(1): 46–53, doi: 10.11840/j.issn.1001-6392.2016.01.007

Garfinkel C I, Schwartz C, Domeisen D I V, et al. 2018. Extratropical atmospheric predictability from the quasi-biennial oscillation in subseasonal forecast models. Journal of Geophysical Research: Atmospheres, 123(15): 7855–7866, doi: 10.1029/2018JD028724

Geng Quanzhen, Sugi M. 2001. Variability of the North Atlantic cyclone activity in winter analyzed from NCEP-NCAR reanalysis data. Journal of Climate, 14(18): 3863–3873, doi: 10.1175/1520-0442(2001)014<3863:VOTNAC>2.0.CO;2

Ghatak D, Frei A, Gong G, et al. 2010. On the emergence of an Arctic amplification signal in terrestrial Arctic snow extent. Journal of Geophysical Research: Atmospheres, 115(D24): D24105, doi: 10.1029/2010JD014007

Gong G, Entekhabi D, Cohen J. 2002. A large-ensemble model study of the wintertime AO-NAO and the role of interannual snow perturbations. Journal of Climate, 15(23): 3488–3499, doi: 10.1175/1520-0442(2002)015<3488:ALEMSO>2.0.CO;2

Graham N E, Diaz H F. 2001. Evidence for intensification of North Pacific winter cyclones since 1948. Bulletin of the American Meteorological Society, 82(9): 1869–1894, doi: 10.1175/1520-0477(2001)082<1869:EFIONP>2.3.CO;2

Guo Yanjuan, Shinoda T, Lin Jialin, et al. 2017. Variations of northern hemisphere storm track and extratropical cyclone activity associated with the Madden-Julian oscillation. Journal of Climate, 30(13): 4799–4818, doi: 10.1175/JCLI-D-16-0513.1

Haak U, Ulbrich U. 1996. Verification of an objective cyclone climatology for the North Atlantic. Meteorologische Zeitschrift, 5, 24–30. https://doi.org/10.1127/metz/5/1996/24

Hall R, Erdélyi R, Hanna E, et al. 2015. Drivers of North Atlantic polar front jet stream variability. International Journal of Climatology, 35(8): 1697–1720, doi: 10.1002/joc.4121

Hannachi A, Jolliffe I T, Stephenson D B. 2007. Empirical orthogonal functions and related techniques in atmospheric science: a review. International Journal of Climatology, 27(9): 1119–1152, doi: 10.1002/joc.1499

Haurwitz M W, Brier G W. 1981. A critique of the superposed epoch analysis method: its application to solar-weather relations. Monthly Weather Review, 109(10): 2074–2079, doi: 10.1175/1520-0493(1981)109<2074:ACOTSE>2.0.CO;2

Haynes P H, McIntyre M E, Shepherd T G, et al. 1991. On the "Downward Control" of extratropical diabatic circulations by eddy-induced mean zonal forces. Journal of the Atmospheric Sciences, 48(4): 651–678, doi: 10.1175/1520-0469(1991)048<0651:OTCOED>2.0.CO;2

Hersbach H, Bell B, Berrisford P, et al. 2020. The ERA5 global reanalysis. Quarterly Journal of the Royal Meteorological Society, 146(730): 1999–2049, doi: 10.1002/qj.3803

Hoskins B J, Hodges K I. 2002. New perspectives on the Northern Hemisphere winter storm tracks. Journal of the Atmospheric Sciences, 59(6), 1041–1061

Kalman D. 1996. A singularly valuable decomposition: the SVD of a matrix. The College Mathematics Journal, 27(1): 2–23, doi: 10.1080/07468342.1996.11973744

Kaplan A. 2011. Sidebar 1. 1: patterns and indices of climate variability [in "State of the Climate in 2010"]. BAMS, 92(6): S20-S25

Kidston J, Scaife A A, Hardiman S C, et al. 2015. Stratospheric influence on tropospheric jet streams, storm tracks and surface weather. Nature Geoscience, 8(6): 433–440, doi: 10.1038/NGEO2424

Knippertz P, Ulbrich U, Speth P. 2000. Changing cyclones and surface wind speeds over the North Atlantic and Europe in a transient GHG experiment. Climate Research, 15(2): 109–122

Kobashi F, Doi H, Iwasaka N. 2019. Sea surface cooling induced by extratropical cyclones in the subtropical North Pacific: Mechanism and interannual variability. Journal of Geophysical Research: Oceans, 124(3): 2179–2195

Laken B A, Čalogović J. 2013. Composite analysis with Monte Carlo methods: an example with cosmic rays and clouds. Journal of Space Weather and Space Climate, 3: A29, doi: 10.1051/swsc/2013051

Lee Y Y, Lim G H. 2012. Dependency of the North Pacific winter storm tracks on the zonal distribution of MJO convection. Journal of Geophysical Research: Atmospheres, 117(D14): D14101, doi: 10.1029/2011JD016417

Lionello P, Boldrin U, Giorgi F. 2008. Future changes in cyclone climatology over Europe as inferred from a regional climate simulation. Climate Dynamics, 30, 657–671. https://doi.org/10.1007/s00382-007-0315-0

Luo Dehai, Cha Jing, Feldstein S B. 2012. Weather regime transitions and the interannual variability of the north Atlantic oscillation. Part I: a likely connection. Journal of the Atmospheric Sciences, 69(8): 2329–2346, doi: 10.1175/JAS-D-11-0289.1

Luo Dehai, Gong Tingting, Diao Yina. 2007. Dynamics of eddy-driven low-frequency dipole modes. Part III: meridional displacement of westerly jet anomalies during two phases of NAO. Journal of the Atmospheric Sciences, 64(9): 3232–3248, doi: 10.1175/JAS3998.1

Ma C G, Chang E K M. 2017. Impacts of storm-track variations on wintertime extreme weather events over the continental United States. Journal of Climate, 30(12): 4601–4624, doi: 10.1175/JCLI-D-16-0560.1

Marshall A G, Scaife A A, Ineson S. 2009. Enhanced seasonal prediction of European winter warming following volcanic eruptions. Journal of Climate, 22(23): 6168–6180, doi: 10.1175/2009JCLI3145.1

Maycock A C, Keeley S P E, Charlton-Perez A J, et al. 2011. Stratospheric circulation in seasonal forecasting models: implications for seasonal prediction. Climate Dynamics, 36(1): 309–321, doi: 10.1007/s00382-009-0665-x

Mendes D, Souza E P, Marengo J A, Mendes M C D. 2010. Climatology of extratropical cyclones over the South American-southern oceans sector. Theoretical and Applied Climatology, 100: 239–250, https://doi.org/10.1007/s00704-009-0161-6

Overland J E, Wang M. 2010. Large-scale atmospheric circulation changes are associated with the recent loss of Arctic sea ice. Tellus A: Dynamic Meteorology and Oceanography, 62(1), 1–9

Pinto J G, Spangehl T, Ulbrich U, et al. 2006. Assessment of winter cyclone activity in a transient ECHAM4-OPYC3 GHG experiment. Meteorologische Zeitschrift, 15(3): 279–291, doi: 10.1127/0941-2948/2006/0128

Pinto J G, Ulbrich U, Leckebusch G C, et al. 2007. Changes in storm track and cyclone activity in three SRES ensemble experiments with the ECHAM5/MPI-OM1 GCM. Climate Dynamics, 29(2): 195–210, doi: 10.1007/s00382-007-0230-4

Raible C C. 2007. On the relation between extremes of midlatitude cyclones and the atmospheric circulation using ERA40. Geophysical Research Letters, 34(7): L07703, doi: 10.1029/2006GL029084

Rayner N A, Parker D E, Horton E B, et al. 2003. Global analyses of sea surface temperature, sea ice, and night marine air temperature since the late nineteenth century. Journal of Geophysical Research: Atmospheres, 108(D14): 4407, doi: 10.1029/2002JD002670

Sanders F, Gyakum J R. 1980. Synoptic-dynamic climatology of the "Bomb". Monthly Weather Review, 108(10): 1589–1606, doi: 10.1175/1520-0493(1980)108<1589:SDCOT>2.0.CO;2

Scaife A A, Spangehl T, Fereday D R, et al. 2012. Climate change projections and stratosphere-troposphere interaction. Climate Dynamics, 38(9–10): 2089–2097, doi: 10.1007/s00382-011-1080-7

Serreze M C, Carse F, Barry R G, et al. 1997. Icelandic low cyclone activity: climatological features, linkages with the NAO, and relationships with recent changes in the Northern Hemisphere circulation. Journal of Climate, 10(3): 453–464, doi: 10.1175/1520-0442(1997)010<0453:ILCACF>2.0.CO;2

Tian Di, Wood E F, Yuan Xing. 2017. CFSv2-based sub-seasonal precipitation and temperature forecast skill over the contiguous United States. Hydrology and Earth System Sciences, 21(3):

1477–1490, doi: 10.5194/hess-21-1477-2017

Trenberth K E, Hurrell J W. 1994. Decadal atmosphere-ocean variations in the Pacific. Climate Dynamics 9, 303–319.

Vihma T. 2014. Effects of arctic sea ice decline on weather and climate: a review. Surveys in Geophysics, 35(5): 1175–1214, doi: 10.1007/s10712-014-9284-0

Wallace J M, Lim G H, Blackmon M L. 1988. Relationship between cyclone tracks, anticyclone tracks and baroclinic waveguides. Journal of the Atmospheric Sciences, 45(3): 439–462, doi: 10.1175/1520-0469(1988)045<0439:RBCTAT>2.0.CO;2

Walter K, Graf H F. 2005. The North Atlantic variability structure, storm tracks, and precipitation depending on the polar vortex strength. Atmospheric Chemistry and Physics, 5(1): 239–248, doi: 10.5194/acp-5-239-2005

Wu Bingyi, Zhang Renhe, D'Arrigo R, et al. 2013. On the relationship between winter sea ice and summer atmospheric circulation over Eurasia. Journal of Climate, 26(15): 5523–5536, doi: 10.1175/JCLI-D-12-00524.1

Xiang Baoqiang, Lin S J, Zhao Ming, et al. 2019. Subseasonal week 3–5 surface air temperature prediction during boreal wintertime in a GFDL model. Geophysical Research Letters, 46(1): 416–425, doi: 10.1029/2018GL081314

Yang Minghao, Li Chongyin, Luo Dehai, et al. 2022. Mechanical and thermal impacts of the Tibetan-Iranian plateau on the North Pacific storm track: numerical experiments by FGOALS-f3-L. Journal of Geophysical Research: Atmospheres, 127(11): e2021JD035659, doi: 10.1029/2021JD035659

Yau A M W, Chang E K M. 2020. Finding storm track activity metrics that are highly correlated with weather impacts. Part I: frameworks for evaluation and accumulated track activity. Journal of Climate, 33(23): 10169–10186, doi: 10.1175/JCLI-D-20-0393.1

Yoshida A, Asuma Y. 2004. Structures and environment of explosively developing extratropical cyclones in the northwestern Pacific region. Monthly Weather Review, 132(5): 1121–1142, doi: 10.1175/1520-0493(2004)132<1121:SAEOED>2.0.CO;2

Zhang Yingxian, Ding Yihui, Li Qiaoping. 2012. Interdecadal variations of extratropical cyclone activities and storm tracks in the Northern Hemisphere. Chinese Journal of Atmospheric Sciences (in Chinese), 36(5): 912–928, doi: 10.3878/j.issn.1006-9895.2012.11158

Zhang Yunqing, Held I M. 1999. A linear stochastic model of a GCM's midlatitude storm tracks. Journal of the Atmospheric Sciences, 56(19): 3416–3435, doi: 10.1175/1520-0469(1999)056<3416:ALSMOA>2.0.CO;2